International Journal of Power System Operation and Energy Management

Volume 2 | Issue 2 Article 3

April 2013

INFLUENCE OF TCSC FACTS DEVICE ON STEADY STATE VOLTAGE STABILITY

Gaber El-saady
Assiut University, Assiut, Egypt, gaber1@yahoo.com

MOHAMED A. A. Wahab
Electrical Engineering Department Minia University, Minia, Egypt, ma_abdelwahab1@hotmail.com

M. F. Basheer
Electrical Engineering Department Minia University, Minia, Egypt, mfarouk3000@yahoo.com

INFLUENCE OF TCSC FACTS DEVICE ON STEADY STATE VOLTAGE STABILITY

[1]GABER EL-SAADY, [2]MOHAMED A. A. WAHAB, [3]MOHAMED M. HAMADA, [4]M. F. BASHEER

[1]Electrical Engineering Department Assiut University, Assiut, Egypt
[2, 3&4]Electrical Engineering Department Minia University, Minia, Egypt
E-mail: gaber1@yahoo.com
ma_abdelwahab1@hotmail.com, mohamed_m-hamad-a@yahoo.co.uk, mfarouk3000@yahoo.com

Abstract— The influence of series Flexible AC Transmission Systems (FACTS) device namely, Thyristor-Controlled Series Capacitors (TCSC) on the steady state voltage stability is the main objective of this paper. The Line stability Index LSI under excepted lines outage contingencies is used to identify the critical line which is considered as the best location for TCSC. A modal analysis is used to define the weakest bus of the studied system. The FACTS device is implemented and included into the Newton-Raphson power flow algorithm, and the control function is formulated to achieve the voltage stability enhancement goal. The analysis is preformed on standard IEEE 30 bus system. The proposed scheme are tested under different loading conditions and different nonlinear voltage dependent loads. The simulation results demonstrate the feasibility and effectiveness of the device and the proposed algorithm.

Keywords-*voltage stability; TCSC; FACTS; voltage dependent load*

I. INTRODUCTION

The utilities interest about the voltage instability and voltage collapse problems increase due to structural changes in the electrical sector, such as those caused by privatization and deregulation, modification of the network topology, as well as ever increasing in load demands brought by economic and environmental pressures that led the power systems to operate near its stability limits. Several blackouts are reported in many countries relate to voltage stability problem [1]. As an example, there are six blackouts during six weeks affecting millions of people in US, Sweden, UK, and Denmark [2].

Generally, voltage collapse is the process by which the sequence of events accompanying voltage instability leads to a low unacceptable voltage profile in a significant part of the power system. Voltage collapse may be a possible outcome of voltage instability, which is defined as the attempt of load dynamics to restore power consumption beyond the capability of the combined transmission and generation system [3].

A large number of researchers have been studied the voltage stability problem. Their attention has resulted with a numerous number of papers, books, and reports being published. Most of these are reported in the extensive bibliography [4].

The voltage instability may be classified into transient and steady state, the latest is the main concern in this paper. Steady state voltage stability or Small-disturbance voltage stability refers to the system's ability to maintain steady voltages when subjected to small perturbations such as incremental changes in system load [5].

Many of measures used to prevent voltage instability [6] such as, (i) Placement of series and shunt capacitors, (ii) Generation rescheduling, (iii) Installation of synchronous condensers, (iv) Under-Voltage load shedding, (v) Blocking of Tap-Changer under reverse operation, (vi) Placement of FACTS controllers. The last method is considered in this study.

FACTS is a terminology that embrace a wide range of power electronics controllers. These devices use no delay and high current power electronic devices available today for safe and accurate responses. They are able to control the parameters such as voltage magnitudes and their angles, line impedances, active and reactive power flows [7].

There are many types of FACTS such as, Superconducting magnetic energy storage (SMES), Static Var Compensator (SVC), Static Synchronous Compensator (STATCOM), Static Synchronous Series Compensator (SSSC), Thyristor Controlled Series Capacitor (TCSC), Interline Power Flow Controller (IPFC), and Unified Power Flow controller (UPFC).

TCSC is considered in this paper to enhance steady state voltage stability by incorporate the device into the Newton-Raphson process under different types of voltage dependent loads.

The rest of this paper is structured as follows. In section II, the concept of the steady state voltage stability model is introduced. The structure and operation principles of TCSC is presented in section III. In section IV, the detailed static voltage stability model of TCSC is described. The mathematical model of the voltage dependent loads is explained in section V. In section VI the proposed methodology for the best placement of TCSC is considered. The results obtained for the test system is given and discussed in Section VII. Finally, Section VIII contains the conclusion.

II. STEADY STATE VOLTAGE STABILITY

The steady state (static) analysis methods mainly depend on the steady state model, such as power flow model or a linearized dynamic model described by the steady state operation. These methods [8-10] can be divided into:

1. Load flow feasibility methods, which depend on the existence of an acceptable voltage profile across the network. This approach is concerned with the maximum power transfer capability of the network or the existence of a solved load flow case. There are many criteria proposed under this approach. Some of these criteria are the following:

- The reactive power capability (Q-V curve).
- Maximum power transfer limit (P-V curve).
-Voltage stability proximity index (VSI) or the load flow feasibility index (LFF index).

2. Steady state stability methods, which test the existence of a stable equilibrium operating point of the power system. Some of the criteria proposed under this approach are:

- Eigenvalues of linearized dynamic equations.
- Singular value of Jacobian matrix (SVJ).
- Sensitivity matrices.

The maximum power transfer limit (P-V curve) method is used here as a measure for voltage stability. The procedures used to study the influence of TCSC on the static voltage stability begin with the power flow as the first step.

The power flow model is used to study steady state voltage stability since the power flow equation yield adequate results, as singularities in related power flow Jacobian can be associated with actual singular bifurcation of the corresponding dynamical system [11].

The Newton-Raphson power flow equation represented by:

$$\begin{bmatrix}\Delta P\\ \Delta Q\end{bmatrix}=\begin{bmatrix}J_{11} & J_{12}\\ J_{21} & J_{22}\end{bmatrix}\begin{bmatrix}\Delta\theta\\ \Delta V\end{bmatrix}=J\begin{bmatrix}\Delta\theta\\ \Delta V\end{bmatrix} \quad (1)$$

The power flow model for voltage stability analysis is represented by:

$$F(x,\lambda)=\begin{bmatrix}\Delta P(x,\lambda)\\ \Delta Q(x,\lambda)\end{bmatrix}=0 \quad (2)$$

where $F(x,\lambda)$ is power flow equation and λ is Loading Factor (LF) or system load change that drives the system to collapse in the following way:

$$\begin{aligned} P_{D,i} &= \lambda_{P,i} P_{D0,i}\\ Q_{D,i} &= \lambda_{Q,i} Q_{D0,i} \end{aligned} \quad (3)$$

where $P_{D0,i}$ and $Q_{D0,i}$ represent the initial active and reactive loads at bus i and constants λ_{Pi} and λ_{Qi} respectively represent the active and reactive load increase direction of bus i .

Wherever Times is specified, Times Roman or Times New Roman may be used. If neither is available on your word processor, please use the font closest in appearance to Times. Avoid using bit-mapped fonts if possible. True-Type 1 or Open Type fonts are preferred. Please embed symbol fonts, as well, for math, etc.

Wherever Times is specified, Times Roman or Times New Roman may be used. If neither is available on your word processor, please use the font closest in appearance to Times. Avoid using bit-mapped fonts if possible. True-Type 1 or Open Type fonts are preferred. Please embed symbol fonts, as well, for math, etc.

III. STRUCTURE AND OPERATION PRINCIPLES OF TCSC

Thyristor controlled series compensator (TCSC) is one of the most popular FACTS controllers, which allows rapid and continuous modulation of the transmission line impedance [12]. TCSC vary the electrical length of the compensated transmission line which enables it to be used to provide fast active power flow regulation [7]. It is also, provides powerful means of controlling and increasing power transfer level of a system by varying the apparent impedance of a specific transmission line [13].

The basic structure of TCSC is a thyristor controlled reactor (TCR) connected in parallel with a capacitor as shown in Fig. 1

\

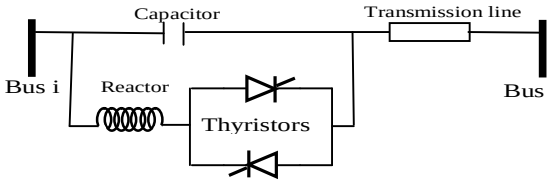

Figure 1. Schematic diagram of TCSC between bus *i* and bus *j*.

The impedance characteristics curve of a TCSC device is shown in Fig. 2, that is drawn between effective reactance of TCSC and firing angle α [14,15].

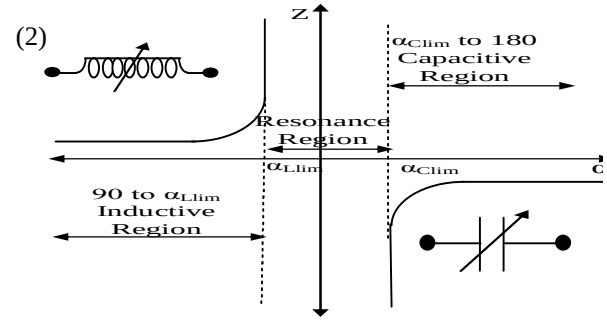

Figure 2. Impedance characteristics curve of a TCSC.

Impedance characteristics of TCSC shows, both capacitive and inductive region are possible through varying firing angle (α) as follows:

$90 < \alpha < \alpha_{Llim}$ Inductive region

$\alpha_{Llim} < \alpha < \alpha_{Clim}$ Capacitive region
$\alpha_{Clim} < \alpha < 180$ Resonance region
While The maximum and minimum value of firing angles should be selected in such a way as to avoid the TCSC operating in high impedance region (at resonance) which results in high voltage drop across the TCSC. This limitation can be used as a constraint during load flow analysis [7].

IV. MODELING OF TCSC CONTROLLER FOR STATIC VOLTAGE STABILITY

For static applications, FACTS devices can be modeled by power injection models (PIM) [16]. The injection model describes FACTS as devices that inject a certain amount of active and reactive power to a node, so that a FACTS device is represented as PQ elements. The advantages of the PIM are that it does not destroy the symmetrical structure of the admittance matrix and allows efficient and convenient integration of FACTS devices into existing power system analytical tools [17].

Fig. 3 shows a model of transmission line with a TCSC connected between buses *k* and *m*. During a steady state, the TCSC can be considered as a reactance $-jX_{TCSC}$. The controllable reactance X_{TCSC} is directly used as the control variable in the power flow equations.

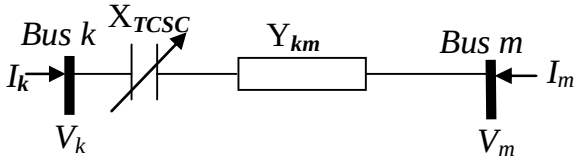

Figure 3. Modeling of transmission line with TCSC.

The current through the line after inserting TCSC is obtained by:

$$I_{km} = (V_k - V_m) / [R_{km} + j(X_{km} - X_{Tc\,sc})]$$

The series capacitor is initially represented as a current dependent voltage source, which is later transformed into a current source Is in parallel with the line [18] where,

$$I_s = -jX_{Tc\,sc} I_{km} / (R_{km} + jX_{km}) \quad (5)$$

The corresponding power injection model of the TCSC incorporated within the transmission line is shown in Fig. 4 The injected powers S_k^F and S_m^F are defined by :

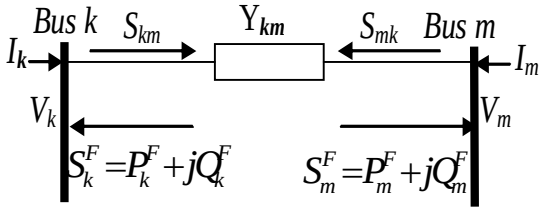

Figure 4. TCSC injection model.

$$S_k^F = V_k(-I_s)^* = V_k\left(\frac{jX_{Tc\,sc}}{R_{km}+jX_{km}}\frac{V_k - V_m}{R_{km}+j(X_{km}-X_{Tc\,sc})}\right)^* \quad (6)$$

$$S_m^F = V_m(I_s)^* = V_m\left(\frac{-jX_{Tc\,sc}}{R_{km}+jX_{km}}\frac{V_k - V_m}{R_{km}+j(X_{km}-X_{Tc\,sc})}\right)^* \quad (7)$$

The real and reactive power injections due to the series capacitor of TCSC at buses *k* and *m* are given by (8) to (11) [19]:

$$P_k^F = V_k^2 G_{kk}^F - V_k V_m [G_{km}^F \cos\delta_{km} + B_{km}^F \sin\delta_{km}] \quad (8)$$

$$Q_k^F = -V_k^2 B_{kk}^F - V_k V_m [G_{km}^F \sin\delta_{km} - B_{km}^F \cos\delta_{km}] \quad (9)$$

$$P_m^F = V_m^2 G_{mm}^F - V_k V_m [G_{km}^F \cos\delta_{km} + B_{km}^F \sin\delta_{km}] \quad (10)$$

$$Q_m^F = -V_m^2 B_{mm}^F - V_k V_m [G_{km}^F \sin\delta_{km} - B_{km}^F \cos\delta_{km}] \quad (11)$$

Where,

$$G_{kk}^F = \frac{X_{Tc\,sc} R_{km}(X_{Tc\,sc} - 2X_{km})}{(R_{km}^2 + X_{km}^2)(R_{km}^2 + (X_{km} - X_{Tc\,sc})^2)}$$

$$B_{kk}^F = \frac{-X_{Tc\,sc}(R_{km}^2 - X_{km}^2 + X_{Tc\,sc}X_{km})}{(R_{km}^2 + X_{km}^2)(R_{km}^2 + (X_{km} - X_{Tc\,sc})^2)}$$

$$G_{mm}^F = -G_{km}^F = G_{kk}^F \quad (4)$$

$$B_{mm}^F = -B_{km}^F = B_{kk}^F$$

To implement voltage control function model of TCSC in Newton-Raphson algorithm, there are two model of TCSC. In the first one, X_{Tcsc} is considered as the state variable, Where the series reactance is adjusted automatically, within limits, to satisfy a specified amount of active power flows through it. In the second model TCSC firing angle is chosen to be the state variable in the Newton–Raphson power flow solution. Where TCSC reactance–firing-angle characteristic, given in the form of a nonlinear relation. The first model is used in this study.

To improve the static voltage stability, The bus voltage control mode is used , So the bus voltage control constraint of bus *k* is given by

$$VC = V_k - V_k^{sp} = 0 \quad (12)$$

Where V_k^{sp} is the bus voltage control reference

After insert TCSC between bus *k* and bus *m*, The power flow relationship is changed to be as :

$$\begin{bmatrix} \Delta P_h \\ \Delta P_k \\ \Delta P_m \\ \Delta Q_h \\ \Delta Q_k \\ \Delta Q_m \\ \cdots\cdots \\ \Delta VC \end{bmatrix} = \begin{bmatrix} \frac{\partial P_h}{\partial \theta_h} & \frac{\partial P_h}{\partial \theta_k} & \frac{\partial P_h}{\partial \theta_m} & \frac{\partial P_h}{\partial V_h} & \frac{\partial P_h}{\partial V_k} & \frac{\partial P_h}{\partial V_m} & \frac{\partial P_h}{\partial X_{Tcsc}} \\ \frac{\partial P_k}{\partial \theta_h} & \frac{\partial P_k^F}{\partial \theta_k} & \frac{\partial P_k^F}{\partial \theta_m} & \frac{\partial P_k}{\partial V_h} & \frac{\partial P_k^F}{\partial V_k} & \frac{\partial P_k^F}{\partial V_m} & \frac{\partial P_k^F}{\partial X_{Tcsc}} \\ \frac{\partial P_m}{\partial \theta_h} & \frac{\partial P_m^F}{\partial \theta_k} & \frac{\partial P_m^F}{\partial \theta_m} & \frac{\partial P_m}{\partial V_h} & \frac{\partial P_m^F}{\partial V_k} & \frac{\partial P_m^F}{\partial V_m} & \frac{\partial P_m^F}{\partial X_{Tcsc}} \\ \frac{\partial Q_h}{\partial \theta_h} & \frac{\partial Q_h}{\partial \theta_k} & \frac{\partial Q_h}{\partial \theta_m} & \frac{\partial Q_h}{\partial V_h} & \frac{\partial Q_h}{\partial V_k} & \frac{\partial Q_h}{\partial V_m} & \frac{\partial Q_h}{\partial X_{Tcsc}} \\ \frac{\partial Q_k}{\partial \theta_h} & \frac{\partial Q_k^F}{\partial \theta_k} & \frac{\partial Q_k^F}{\partial \theta_m} & \frac{\partial Q_k}{\partial V_h} & \frac{\partial Q_k^F}{\partial V_k} & \frac{\partial Q_k^F}{\partial V_m} & \frac{\partial Q_k^F}{\partial X_{Tcsc}} \\ \frac{\partial Q_m}{\partial \theta_h} & \frac{\partial Q_m^F}{\partial \theta_k} & \frac{\partial Q_m^F}{\partial \theta_m} & \frac{\partial Q_m}{\partial V_h} & \frac{\partial Q_m^F}{\partial V_k} & \frac{\partial Q_m^F}{\partial V_m} & \frac{\partial Q_m^F}{\partial X_{Tcsc}} \\ \cdots & \cdots & \cdots & \cdots & \cdots & \cdots & \cdots \\ \frac{\partial VC}{\partial \theta_h} & \frac{\partial VC}{\partial \theta_k} & \frac{\partial VC}{\partial \theta_m} & \frac{\partial VC}{\partial V_h} & \frac{\partial VC}{\partial V_k} & \frac{\partial VC}{\partial V_m} & \frac{\partial VC}{\partial X_{Tcsc}} \end{bmatrix} \begin{bmatrix} \Delta\theta_h \\ \Delta\theta_k \\ \Delta\theta_m \\ \Delta V_h \\ \Delta V_k \\ \Delta V_m \\ \cdots\cdots \\ \Delta X_{Tcsc} \end{bmatrix} \quad (13)$$

Where,

h :2,3,…,n

Equation (13) is a modification of (1), which represent Newton-Raphson power flow equation with TCSC.

V. MATHEMATICAL MODELS OF VOLTAGE DEPENDENT LOADS

A static model expresses the active and reactive powers at any instant in time as functions of the bus voltage magnitude and frequency at the same instant. Static load model is used both for essentially static load components (e.g., resistive and lighting loads), and as an approximation for dynamic load components [20].

The exponential function of voltage can be expressed in terms of nominal operating point designed by the subscripts "$_0$".

$$P_L = P_0\left(\frac{V}{V_0}\right)^{\alpha}$$

$$Q_L = Q_0\left(\frac{V}{V_0}\right)^{\beta} \quad (14)$$

where, P_L, Q_L are load active and reactive power, P_0 ,Q_0 are active and reactive power consumption at rated voltage V_0, α is the active power exponent, β is the reactive power exponent, V is the bus voltage , and V_0 is the rated voltage

There are three types of static load modeling depending on the values of α and β as follows:

Constant current model: When α and β equal 1, the static model power varies directly with voltage variation.

Constant impedance model: When α and β equal 2, the static load model power varies directly with the square of voltage magnitude.

Constant power model: When α and β equal zero the static model power is constant in spite of voltage magnitude variations. It's also called a constant MVA model.

VI. BEST PLACEMENT METHODOLOGY FOR TCSC FACTS DEVICE

To determine the best location of TCSC device, the proposed methodology begin with identifying the critical line using LSI during line outage contingency. Then, modal analysis is utilized to define the weakest bus, to form the voltage control function, These procedures are done as follows:

A. Identifying Critical Line Using LSI and Line Outage Contingency Analysis

When a line outage occurs the Jacobian matrix needs to be modified to reflect the outage effect [21]. To make such modification a nominal circuit of an outage line *i-j* is presented in Fig. 5. The two power injections and which represent the effect of the outage [22].

The outage effect is simulated by making the two power injection and equal to the power flows on the outage line with opposite signs. Therefore,

$$S_{ci} = P_{ci} + jQ_{ci} = jY_C V_i^2 - V_i^2 |Y_S| e^{j\delta_s} + V_i V_j |Y_S| e^{j(\delta_s + \theta_i - \theta_j)} \quad (15)$$

$$S_{cj} = P_{cj} + jQ_{cj} = jY_C V_j^2 - V_j^2 |Y_S| e^{j\delta_s} + V_i V_j |Y_S| e^{j(\delta_s + \theta_j - \theta_i)} \quad (16)$$

$$P_{ci} = V_i V_j |Y_S| \cos(\delta_s + \theta_i - \theta_j) - V_i^2 |Y_S| \cos\delta_s \quad (17)$$

$$Q_{ci} = V_i V_j |Y_S| \sin(\delta_s + \theta_i - \theta_j) - V_i^2 |Y_S| \sin\delta_s + Y_C V_i^2 \quad (18)$$

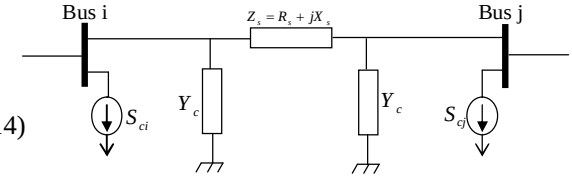

Figure 5. Line outage power injection model for line *i-j*

$$P_{cj} = V_i V_j |Y_S| \cos(\delta_s + \theta_j - \theta_i) - V_j^2 |Y_S| \cos\delta_s \quad (19)$$

$$Q_{cj} = V_i V_j |Y_S| \sin(\delta_s + \theta_j - \theta_i) - V_j^2 |Y_S| \sin\delta_s + Y_C V_j^2 \quad (20)$$

where $Y_s = 1/Z_s = |Y_s| e^{-j\delta s}$

Using (17) to (20) the Jacobian matrix form in (1) is modified to reflect the effects of the active and reactive power injections at buses *i* and *j*. Totally 16 elements need to be modified, and they are combined together to form the matrix ΔJ

$$\Delta J = \begin{bmatrix} \Delta\frac{\partial P_i}{\partial \theta_i} & \Delta\frac{\partial P_i}{\partial \theta_j} & \Delta\frac{\partial P_i}{\partial V_i} & \Delta\frac{\partial P_i}{\partial V_j} \\ \Delta\frac{\partial P_j}{\partial \theta_i} & \Delta\frac{\partial P_j}{\partial \theta_j} & \Delta\frac{\partial P_j}{\partial V_i} & \Delta\frac{\partial P_j}{\partial V_j} \\ \Delta\frac{\partial Q_i}{\partial \theta_i} & \Delta\frac{\partial Q_i}{\partial \theta_j} & \Delta\frac{\partial Q_i}{\partial V_i} & \Delta\frac{\partial Q_i}{\partial V_j} \\ \Delta\frac{\partial Q_j}{\partial \theta_i} & \Delta\frac{\partial Q_j}{\partial \theta_j} & \Delta\frac{\partial Q_j}{\partial V_i} & \Delta\frac{\partial Q_j}{\partial V_j} \end{bmatrix} \quad (21)$$

The elements of ΔJ (which are listed in [22]) should be added to their corresponding positions in the original . This process is represented in matrix form as follows:

$$J' = J + M\,\Delta J M^t \quad (22)$$

Where *M* has the following form:

$$M = \begin{bmatrix} N & | & 0 \\ -- & | & -- \\ 0 & | & N \end{bmatrix} \quad (23)$$

Where *0* is *nx2* zero matrix, *N* is a sparse matrix in the form $N=[e_i \quad e_j]$, and e_i , e_j are spares column vectors with only one unity element at position *i* and *j* respectively.

The line stability index LSI is used in this paper in contingency ranking [23]. LSI can be defined by:

$$LSI_{ij} = \frac{R_{ij}P_j + X_{ij}Q_j}{0.25V_i^2} \quad (24)$$

Where R_{ij} , X_{ij} are the resistance and reactance between sending and receiving buses. P_j , Q_j are the reactive and active power at receiving bus. V_i is voltage at sending bus.

The computational procedures are as follows:

i. Base load flow computation is done, and LSI values are computed.
ii. The values of LSI are ranked and the highest values are recorded in list 1.
iii. All lines outages contingencies are simulated by removing each line at a time.
iv. Run load flow program under selected lines outages and reevaluate LSI values for all lines in each case.
v. The highest LSI value from every line outages are selected and registered in List 2
vi. By comparing the two lists the common lines are extracted, and the line outage with highest rank is identified as the best TCSC location .

B. Defining the Weakest Bus of the Network

After defining the proper line to locate TCSC, modal analysis is used to select and assure the weakest bus required to form the voltage control function. Modal or eigenvalues analysis method can predict voltage collapse in complex power system networks. It involves mainly the computing of the smallest eigenvalues and associated eigenvectors of the reduced Jacobian matrix obtained from the load flow solution. the participation factor can be used effectively to find out the weakest nodes or buses in the system [24].

In order to concentrate on the reactive demand and to minimize computational effort by reducing the Jacobian matrix in Newton-Raphson power flow equation represented by (1), ΔP is putted to be zero so

$$\Delta\theta = -J_{11}^{-1}J_{12}\Delta V \quad (25)$$

And

$$\Delta Q = J_{21}\Delta\theta + J_{22}\Delta V \quad (26)$$

From (25) and (26)

$$\Delta Q = J_R \Delta V = [J_{22} - J_{21}J_{11}^{-1}J_{12}]\Delta V \quad (27)$$

Where J_R is the reduced Jacobian matrix of the system.

The eigenvalues and eigenvectors of the reduced order Jacobian matrix J_R are used for the voltage stability characteristics analysis. To detect voltage instability, modes of the eigenvalues matrix J_R is identified. The magnitude of the eigenvalues provides a relative measure of proximity to instability.

Eigenvalue analysis of J_R will be as follows:

$$J_R = \Phi\Lambda\Gamma \quad (28)$$

Where
Φ = right eigenvector matrix of J_R
Γ = left eigenvector matrix of J_R
Λ =diagonal eigenvalue matrix of J_R
And $\Phi\,\Gamma$=1
Equation (28) may be written as:

$$J_R^{-1} = \Phi\Lambda^{-1}\Gamma \quad (29)$$

From (29) and (27) $\Delta V = \Phi\Lambda^{-1}\Gamma\Delta Q$ or

$$\Delta V = \sum_i \frac{\Phi_i \Gamma_i}{\lambda_i}\Delta Q \quad (30)$$

Where is the eigenvalue, is the column right eigenvector and is the row left eigenvector of matrix .

Each i^{th} eigenvalue λ_i and corresponding right and left eigenvectors define the i^{th} mode of the system. The i^{th} modal reactive power variation is defined as:

$$\Delta Q_{mi} = K_i \Phi_i \quad (31)$$

Where K_i is a scale factor to normalize vector ΔQ_i so that

$$K_i^2 \sum_j \Phi_{ji}^2 = 1 \quad (32)$$

With Φ_{ji} the j^{th} element of Φ_i

The corresponding i^{th} modal voltage variation is :

$$\Delta V_{mi} = \frac{1}{\lambda_i} \Delta Q_{mi} \quad (33)$$

Equation (33) indicate that if all the eigenvalues are positive, J_R is positive definite and the V-Q sensitivities are also positive, and the system is voltage stable [25]. The system is considered voltage unstable if at least one of the eigenvalues is negative. A zero eigenvalue of J_R means that the system is close to voltage instability. Furthermore, small eigenvalues of J_R determine the proximity of the system to being voltage unstable. So, Once the minimum eigenvalues and the corresponding left and right eigenvectors have been calculated, the participation factor can be used to identify the weakest node or bus in the system.

The procedure may be summarized as follows:

- Obtain the load flow for the base case of the system and get the Jacobian matrix *J* and the reduced Jacobian J_R
- Compute the eigenvalues to identify how the system close to instability and find the minimum eigenvalue λ_{min} of J_R .
- Calculate the right and left eigenvectors of J_R and compute the participation factors P_{ki} for $(\lambda_{min})_i$. The highest P_{ki} indicate the most participated k^{th} bus to i^{th} mode (which is the closest mode to instability) in the system.
- Generate the Q-V curve to the k^{th} bus. By using Q-V curves, it is possible to know what is the maximum reactive power that can be achieved or added to the weakest bus before reaching minimum voltage limit or voltage instability.

VII. SIMULATION RESULTS

Voltage stability enhancement using the proposed TCSC FACTS device is done through the simulation of IEEE 30- bus test system (shown in Fig. 6). Studied system data is obtained from [26]. All the results are produced by programs developed in MATLAB® software package.

The system consists of 6 machine, 30 bus, and 41 lines. Bus 1 is considered as slack bus, while 5 nodes as PV buses and other buses as PQ buses. For all cases, the convergence tolerance is $1e^{-12}$ p.u. and system base is 100 MVA

As explained in the previous sections LSI under line outage analysis, and modal analysis are used to identify the best location of the TCSC, and the weakest bus required to form the voltage control function, then the TCSC device is incorporated to the system. The effect of the system without and with TCSC is studied under different loading conditions and different load types to investigate the ability of the FACTS device to enhance static voltage stability of the studied system.

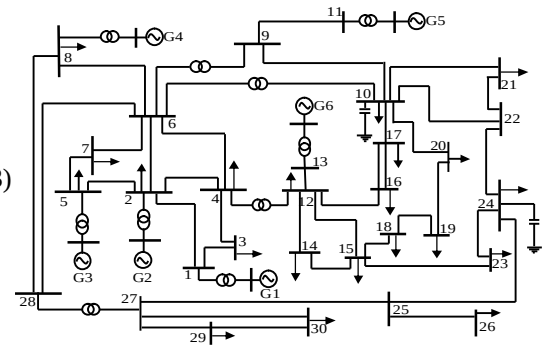

Figure 6. The IEEE 30-bus power system.

A. *Best Location for TCSC Placement*

To define the appropriate placement of TCSC, firstly the base load flow study is carried out, the LSI is computed and ranked, and the most ten severe lines according to LSI values are recorded in Table I. Then the lines outages are simulated and the LSI are computed for each line outage case and the highest LSI value for each case is extracted, and the most serious outage contingency are identified and listed in Table II. The outages of L38 and L39 give non convergence results "NC" and LSI greater than one which mean that these lines cases the system unstable. From the two tables, it is appeared that L38, L39, and L20 are the common lines between the critical lines lists in the base case and in the line outages contingency cases. And the line L38 (the line connecting buses 27-30) is the most critical line which have the highest LSI value. furthermore investigating the LSI values of Table II indicate that the line L38 itself has the highest LSI value under most of the lines contingencies So, the line L38 is chosen to place TCSC device.

TABLE I. THE HIGHEST RANKED LINES ACCORDING TO LSI

Line No	From -To	LSI	Rank
38	L 27-30	0.1765	1
13	L 9-11	0.1722	2
39	L 29-30	0.1378	3
32	L 23-24	0.1159	4
8	L 5-7	0.0907	5
1	L 1-2	0.0904	6
20	L 14-15	0.0867	7
31	L 22-24	0.0864	8
16	L 12-13	0.0822	9
27	L 10-21	0.0752	10

TABLE II. LSI FOR THE STUDIED POWER SYSTEM UNDER DIFFERENT LINES OUTAGE

Line No	Line Outage									
	L1	***L8***	***L13***	***L16***	***L20***	***L27***	***L31***	***L32***	***L38***	***L39***
L1	----	0.0792	0.0797	0.0786	0.0921	0.0793	0.0793	0.0793	NC	NC
L2	0.0109	0.0109	0.0109	0.0109	0.0109	0.0109	0.0109	0.0109	NC	NC
L3	0.0257	0.0261	0.0261	0.0261	0.0261	0.0261	0.0261	0.0261	NC	NC
L4	0.0062	0.0062	0.0062	0.0062	0.0062	0.0062	0.0062	0.0062	NC	NC
L5	0.0758	0.0546	0.0507	0.0521	0.0283	0.0513	0.0513	0.0515	NC	NC
L6	0	0	0	0	0	0	0	0	NC	NC
L7	0	0	0	0	0	0	0	0	NC	NC
L8	0.0907	----	0.0907	0.0907	0.0907	0.0907	0.0907	0.0907	NC	NC
L9	0.0587	0.064	0.0583	0.0583	0.059	0.0583	0.0583	0.0583	NC	NC
L10	0.0099	0.0219	0.0211	0.0193	0.002	0.0202	0.0202	0.0199	NC	NC
L11	0	0	0.1101	0	0	0	0	0	NC	NC
L12	0.0435	0.0432	0.0431	0.0431	0.0437	0.3146	0.0432	0.0432	NC	NC
L13	0.1666	0.1596	----	0.1566	0.1772	0.1603	0.1607	0.1575	NC	NC
L14	0.0081	0.0081	0.0081	0.0081	0.0082	0.0591	0.0081	0.0081	NC	NC
L15	0.0747	0.0747	0.0747	0.043	0.0754	0.0746	0.0747	0.0747	NC	NC
L16	0.077	0.0746	0.0751	----	0.0659	0.0731	0.0734	0.0765	NC	NC
L17	0.0425	0.0424	0.0424	0.0422	0.0684	0.0423	0.0424	0.0424	NC	NC
L18	0.0315	0.0314	0.0314	0.0313	0.0188	0.0314	0.0314	0.0314	NC	NC
L19	0.0249	0.0249	0.0249	0.0248	0.0253	0.0249	0.0249	0.0249	NC	NC
L20	0.0865	0.0864	0.0864	0.086	----	0.0862	0.0863	0.0865	NC	NC
L21	0.0698	0.0696	0.0697	0.0694	0.0705	0.0695	0.0696	0.0696	NC	NC
L22	0.0205	0.0204	0.0204	0.0204	0.0207	0.0204	0.0204	0.0205	NC	NC
L23	0.0408	0.0407	0.0407	0.0405	0.0412	0.0406	0.0407	0.0407	NC	NC
L24	0.0048	0.0048	0.0048	0.0048	0.0049	0.0048	0.0048	0.0048	NC	NC
L25	0.0135	0.0134	0.0134	0.0134	0.0136	0.0134	0.0134	0.0134	NC	NC
L26	0.0299	0.0298	0.0298	0.0297	0.0301	0.0298	0.0298	0.0298	NC	NC
L27	0.0554	0.0552	0.0553	0.0551	0.0558	----	0.0553	0.0551	NC	NC
L28	0	0	0	0	0	0	0.0218	0	NC	NC
L29	0	0	0	0	0	0	0.0035	0	NC	NC
L30	0.0244	0.0243	0.0243	0.0242	0.0246	0.0243	0.0243	0.0543	NC	NC
L31	0.0861	0.0858	0.0859	0.0856	0.0868	0.0847	----	0.058	NC	NC
L32	0.1155	0.1152	0.1153	0.1148	0.1166	0.1146	0.0749	----	NC	NC
L33	0	0	0	0	0	0	0	0	NC	NC
L34	0.0699	0.0695	0.0696	0.0694	0.0704	0.0691	0.0692	0.0692	NC	NC
L35	0	0	0	0	0	0	0	0	NC	NC
L36	0	0	0	0	0	0	0	0	NC	NC
L37	0.0349	0.0347	0.0347	0.0346	0.0351	0.0345	0.0345	0.0346	NC	NC
L38	0.1759	0.1746	0.1746	0.1744	0.1769	0.1738	0.174	0.1741	----	NC
L39	0.1372	0.1362	0.1362	0.136	0.1381	0.1356	0.1357	0.1358	NC	----
L40	0	0	0	0	0	0	0	0	NC	NC
L41	0	0	0	0	0	0	0	0	NC	NC

The highest l e during line outage The critical l ge that case a non converge state

B. Identification of The Weakest Bus

To define the weakest bus, the modal analysis method is applied to the suggested test systems (as in section VI.B). The voltage profile of the buses is presented in Fig. 7.

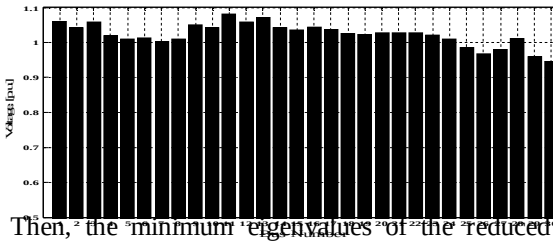

Then, the minimum eigenvalues of the reduced Jacobian matrix are calculated and registered in Table III.

TABLE III. THE EIGENVALUES FOR THE PQ BUSES

Bus No	Eigenvalue	Bus No	Eigenvalue
3	107.48766	19	18.72292
4	100.92729	20	3.59637
6	59.71765	21	4.06940
7	47.33923	22	5.48372
9	37.90579	23	6.04582
10	34.85240	24	16.44144
12	23.35048	25	15.58759
14	22.81107	26	12.90193
15	0.51305	27	13.69709
16	1.03581	28	8.82146
17	1.73317	29	7.48722
18	19.83127	30	5.69517

After that, the weakest load buses, which are subjected to voltage collapse, are identified by computing the participating factors. The results are shown in Fig. 8

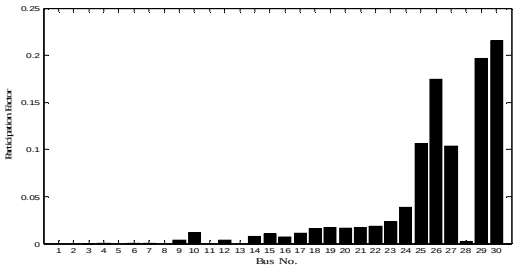

Figure 8. Participation factors for PQ buses

Fig. 7 shows the voltage profile of all buses of the IEEE 30 bus system as obtained form the load flow. It can be seen that all the bus voltages are within the acceptable level (±5%) except bus number 30, which is about 0.944 p.u.

The total number of eigenvalues of the reduced Jacobian matrix J_R is 24, as there are 24 PQ buses. These eigenvalues are shown in Table III. All the eigenvalues are positive which means that the system voltage is stable. It can be noticed that the minimum eigenvalue that equal to 0.513 is the most critical mode. The participating factor for this mode has been calculated and the results are shown in Fig. 8. The results show that, the buses 30, 29 and 26 have the largest participation factors. The highest participation factor value at bus 30 illustrates the remarkable role of this bus in the voltage collapse.

The Q-V curves are depicted in Fig. 9 for the weakest buses of the critical mode as expected by the modal analysis method. The curve verifies the results obtained previously by modal analysis method. It can be seen that buses 30, and 26 are the critical buses compared the bus 29 but with keeping in mind the participation factors bus 30 will be the most critical one. where any more increase in the reactive power demand in that bus will cause a voltage collapse. Therefore Bus 30 is selected to form the voltage control function.

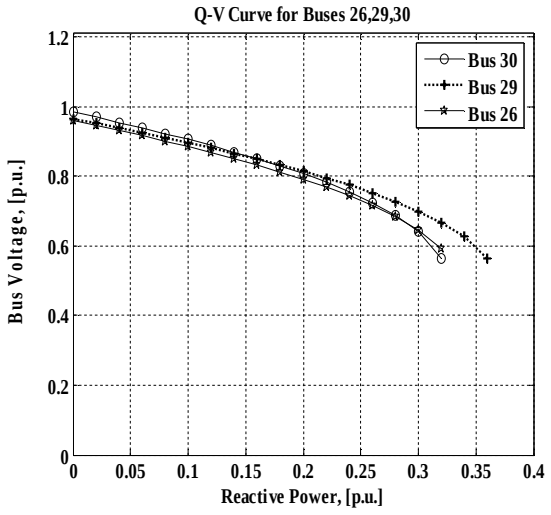

Figure 9. Q-V Curves for critical buses

C. Simulation Results With Effect of TCSC Using Linear Loads

To investigate the effect of the TCSC device suing linear loads (P-constant load), PV curves of the critical buses 30, 29, and 26 without and with TCSC (TCSC at line 27-30) are shown in Fig. 10 to Fig. 12. Fig. 10 indicates that the device succeed to fix the voltage of the most critical bus 30 to the objective value (1 p.u.), despite the increasing of the loading factor to 1.4. Also, Fig.11 and Fig. 12 show an improvement in the voltage profiles in buses 29 and 26. So, all the results are shown that the voltage profiles are enhanced and consequently the voltage stability margin of the studied system are improved due to using TCSC.

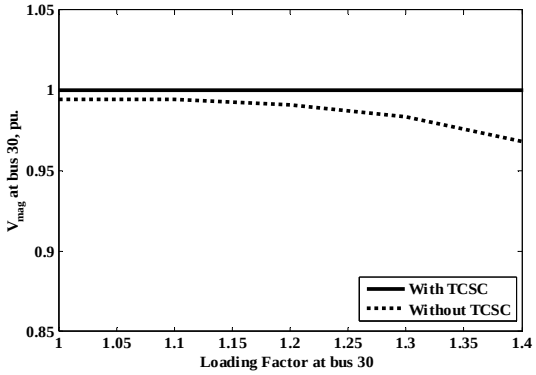

Figure 10. P-V curve of bus 30 without and with TCSC

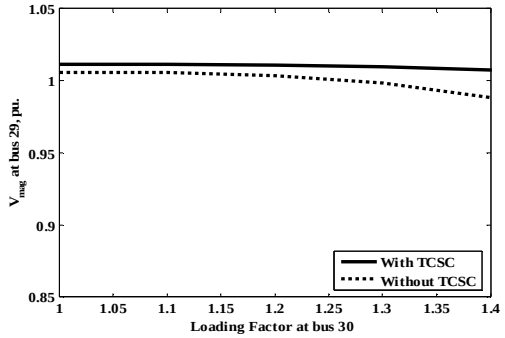

Figure 11. P-V curve of bus 29 without and with TCSC.

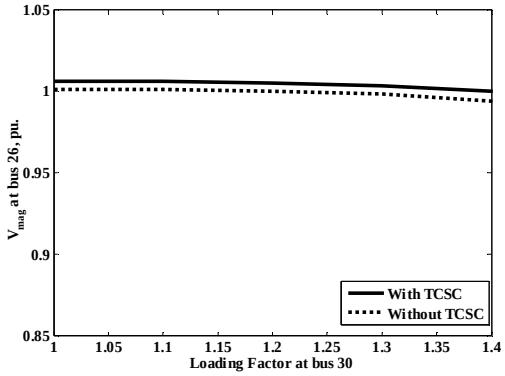

Figure 12. P-V curve of bus 26 without and with TCSC

D. Simulation Results with Effect of TCSC using Voltage Dependent Loads

To explore the effect of the TCSC device on the proposed system under different nonlinear voltage dependent loads, PV curves of the buses 26, 29, and 30 without and with TCSC are plotted in Fig. 13 to Fig. 21. Figures are zoomed when required to explain the case. Also, the loading factor are changed according to case stability.

Figures 13 to 15 simulate the change in voltage magnitude of the three buses in the studied system without TCSC under constant current (CI), constant impedance (CZ), and constant power (CP) loads. These figures indicate that the voltage magnitude are decreased to undesirable levels that lead to voltage collapse.

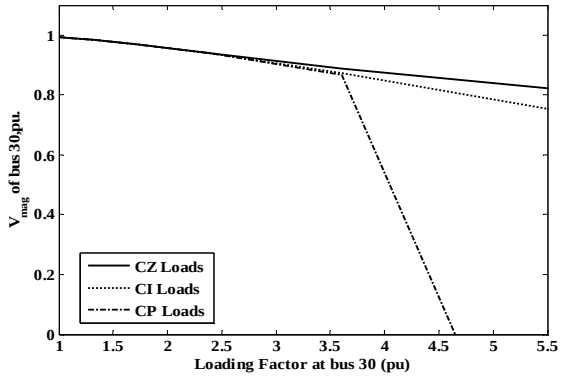

Figure 13. P-V curve of bus 30 for different load types

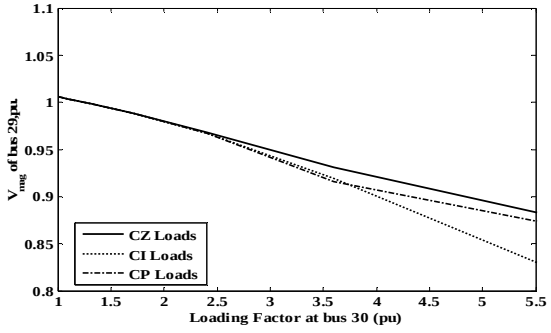

Figure 14. P-V curve of bus 29 for different load types

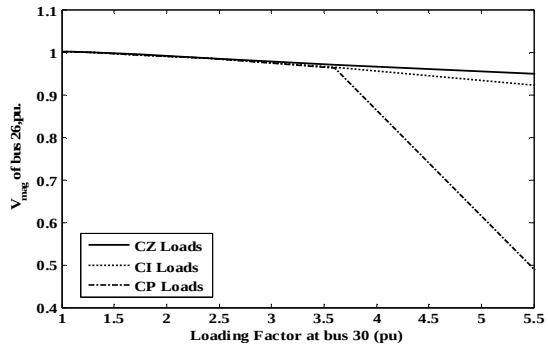

Figure 15. P-V curve of bus 26 for different load types

In figures 16 to 18 a comparison between the system with TCSC and without TCSC using constant current loads are depicted. Also, In figures 19 to 21 the same process is done, using constant impedance load types (constant power case are studied as linear load). In figures 12, 18 and 21 the TCSC has a small effect on bus 26 this is because of bus 26 is not connected directly to bus 30 that is connected to TCSC this means that the redistribution of reactive powers by the device has not a large effect of this bus. In general TCSC shows a good performance and enhance the voltage stability margin of the system.

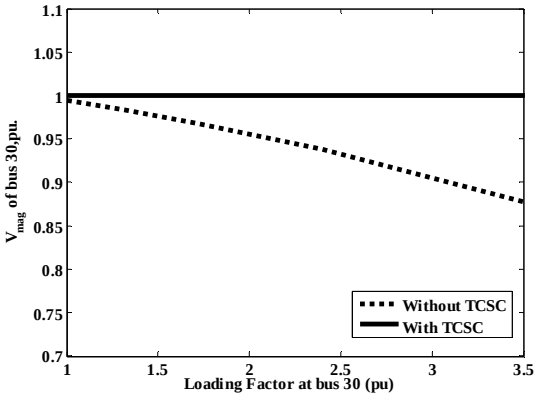

Figure 16. P-V curve of bus 30 for constant current load

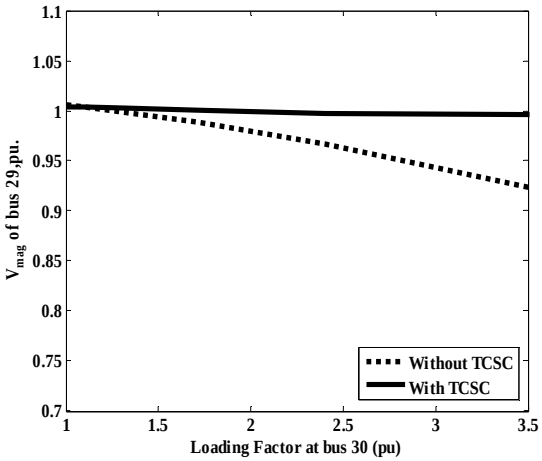

Figure 17. P-V curve of bus 29 for constant current load

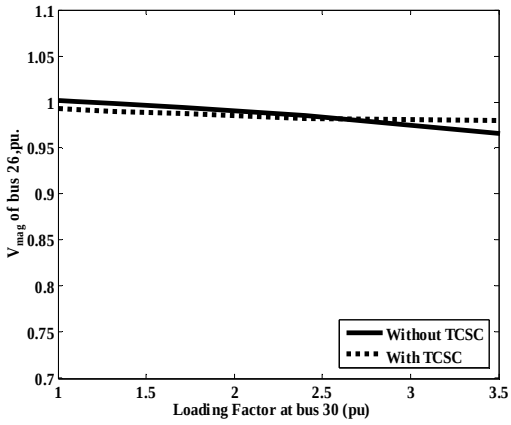

Figure 18. P-V curve of bus 26 for constant current load

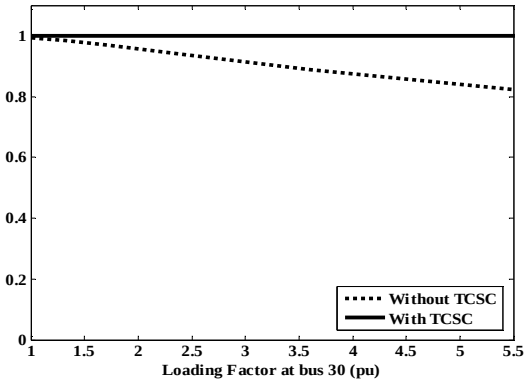

Figure 19. P-V curve of bus 30 for constant impedance load

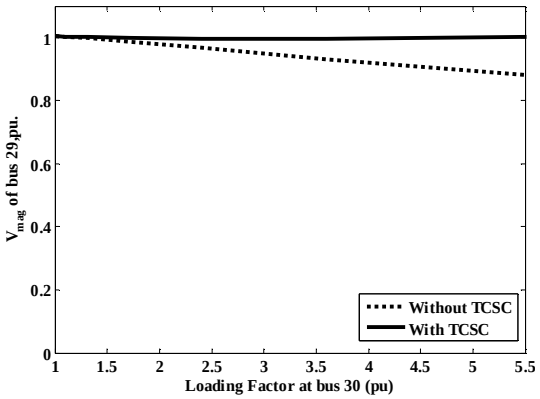

Figure 20. P-V curve of bus 30 for constant impedance load

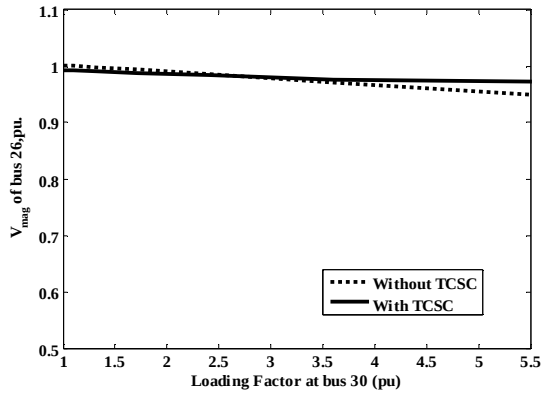

Figure 21. P-V curve of bus 30 for constant impedance load

VIII. CONCLUSION

In this paper the influence of TCSC on steady state voltage stability was investigated. Detailed steady state model of FACTS device was presented focusing on the inclusion of the devices into the power flow analysis process. A novel techniques for selecting best placement of the device and to form the voltage control function were proposed. The studied system was tested under different loading conditions and different linear and nonlinear load types. The device proved their ability to enhance voltage stability margin.

REFERENCES

[1] W. Bialek: Cambridge Working Papers in Economics CWPE 0407, 2004[online] Available:http:// www.dspace.cam.ac.uk/ bitstream/1810-/386/1/EP34.pdf .

[2] Y.V. Makarov, V.I. Reshetov, A. Stroev, and I. Voropai, "Blackout prevention in the United States, Europe, and Russia," Proceedings of the IEEE, vol. 93, no. 11, Nov. 2005, pp. 1942-1955.

[3] T.V Cutsem, "Voltage stability of electric power system", Springer, 1998.

[4] Ajjarapu V., Lee B., "Bibliography on voltage stability," IEEE Trans. Power Syst., vol. 13, no. 1, Feb. 1998, pp. 115-125.

[5] IEEE/CIGRE Joint Task Force on Stability Terms and Definitions, "Definition and classification of power system stability," IEEE Trans. Power Syst., vol. 19, no. 2, May 2004, pp. 1387–1401.

[6] S. Gupta, R.K Tripathi, and R.D. Shukla, "Voltage stability improvement in power systems using facts controllers: State-of-the-art review," Proceedings of International Conference on Power, Control and Embedded Systems (ICPCES), Allahabad, India, Nov. 2010, pp. 1-8.

[7] S. Sreejith, Sishaj P Simon, and M P Selvan, "Power flow analysis incorporating firing angle model based TCSC," Proceedings of 5th International Conference on Industrial and Information Systems (ICIIS 2010), India 2010, Jul 29 - Aug 01, pp. 496-501.

[8] C. W. Taylor, "Power system voltage stability." New York: Mcgraw-Hill, 1994.

[9] V. A. Venikov, V. A. Stroev, V. I. Idelchick, and V. I. Trasov, "Estimation of electric power system steady-state stability in load flow calculation," IEEE Transactions on Power Apparatus and Systems, vol. PAS-94, May/June 1975, pp. 1034-1041.

[10] J. C. Chow, R. Fischl, and H. Yan, " On the evaluation of voltage collapse criteria" IEEE Trans. Power Syst., vol. 5, no.2, May 1990, pp. 612-620.

[11] A. Sode-Yome, N. Mithulananthan, K.Y. Lee, " A Comprehensive comparison of FACTS devices for enhancing static voltage stability," IEEE Power Engineering Society General Meeting, 2007, Florida, USA, June 2007, pp. 1-8.

[12] T. Datta, P. Nagendra, and S. Halder nee Dey, "An Integrated model of modern power system in the presence of TCSC and STATCOM controllers to assess global voltage stability," Joint International Conference on Power Electronics, Drives and Energy Systems (PEDES), New Delhi, India, Dec. 2010, pp. 1-6.

[13] Bindeshwar Singh, "Utilities of differential algebraic equations (DAE) model of SVC and TCSC for operation, control, planning & protection of power system environments," International Journal of Reviews in Computing , vol. 7, Sep. 2011, pp. 55– 63.

[14] Anwar S. Siddiqui, Rashmi Jain, Majid Jamil and Gupta C. P., "Congestion management in high voltage transmission line using thyrister controlled series capacitors (TCSC),"

Journal of Electrical and Electronics Engineering Research, vol. 3, no. 8, Oct. 2011, pp. 151– 161.

[15] S. Meikandasivam, Rajesh Kumar Nema and Shailendra Kumar Jain, "Behavioral study of TCSC device – A MATLAB/Simulink implementation," International Journal of Electronics and Electrical Engineering, vol. 2, no. 10, Oct. 2011, pp. 151– 161.

[16] Naresh Acharya, and Nadarajah Mithulananthan, "Influence of TCSC on congestion and spot price in electricity market with bilateral contract," Electric Power Systems Research , vol. 77, no. 8, Aug. 2007, pp. 1010–1018.

[17] Ying Xiao, Y. H. Song, and Y. Z. Sun, "Power flow control approach to power systems with embedded FACTS devices," IEEE Trans. Power Syst., vol. 17, no. 4, Nov. 2002, pp. 943–950.

[18] Balarko Chaudhuri, and Bikash C. Pal, "Robust damping of multiple swing modes employing global stabilizing signals with a TCSC," IEEE Trans. Power Syst., vol. 19, no. 1, Feb. 2004, pp. 499–506.

[19] K.Vijayakumar, "Optimal location of FACTS devices for congestion management in deregulated power systems," International Journal of Computer Applications, vol. 16, no. 6, Feb. 2011, pp. 29– 37.

[20] IEEE Task Force on Load Representation for Dynamic Performance, "Load representation for dynamic performance analysis," IEEE Trans. Power Syst., vol. 8, no. 2, May 1993, pp. 472–482.

[21] K.L. Lo and Z.J. Meng, "Newton-like method for line outage simulation," IEE Proc. C Gener. Trans. Distrib., vol. 151, no. 2, March 2004, pp. 225-231.

[22] G.B. Jasmon, and C.Y. Chuan, "Performance comparison of two exact outage simulation techniques," IEE Proc. C Gener. Trans. Distrib., vol. 132, no. 6, Nov. 1985, pp. 285–293.

[23] A. Yazdanpanah-Goharrizi, and R. Asghari, "A Novel line stability index (NLSI) for voltage stability assessment of power systems," Proceedings of 7th International Conference on Power Syatems (WSEAS), Beijing, China, Sep. 2007, pp. 164-167.

[24] A. Al-Hinai and M. Choudhry "Voltage collapse prediction for interconnected power system", Proceedings of 33rd North American Power Symposium (NAPS), College Station, TX, Oct. 2001, pp. 201-207.

[25] B. Gao, G.K Morison and P. Kundur, "Voltage stability evaluation using modal analysis", IEEE Trans. Power Syst., vol. 7, no. 4, Nov. 1992, pp. 1529- 1542.

[26] Power System Test Case Archive: [Online] http://www.ee.washingto- n.edu/